Ribozyme Knockdown of the γ-Subunit of Rod cGMP Phosphodiesterase Alters the ERG and Retinal Morphology in Wild-Type Mice

Jianwen Liu,[1] Adrian M. Timmers,[1,2] Alfred S. Lewin,[3,4] and William W. Hauswirth[1,4]

PURPOSE. To generate an animal model of retinal degeneration by using AAV-mediated ribozyme knockdown of the γ-subunit of the rod cGMP phosphodiesterase (PDEγ) mRNA in the retina of wild-type mice.

METHODS. Two hammerhead ribozymes, HRz35 and HRz42, were designed to target the PDEγ gene in wild-type C57BL/6 mice. The efficiency and specificity of the ribozyme cleavage was tested in vitro against three different types of target: short synthetic RNA oligomers, longer targets transcribed from clones, and full-length mRNA from total retinal RNA extracts. After in vitro validation, the ribozymes were cloned and packaged in a recombinant adenoassociated virus (rAAV) containing a proximal 472-bp murine rod opsin promoter (MOPS) to drive ribozyme synthesis. Three-week-old wild-type C57BL/6 mice were injected subretinally with the vectors. For treated versus partner control retinas, responses to light were measured by full-field electroretinography (ERG), and retinal tissues were examined by light microscopy. Messenger RNA and protein levels of PDEγ gene were monitored by reverse transcription–polymerase chain reaction (RT-PCR) and Western immunoblot assay.

RESULTS. The ribozymes had comparable in vitro kinetic properties in multiple turnover kinetic analyses. Ribozyme HRz35 exhibited a K_{cat} of 0.48 minute^{-1} and a K_m of 980 nM, and HRz42 showed a K_{cat} of 0.17 minute^{-1} and a K_m of 971 nM. Both ribozymes cleaved at accessible sites in the RNA, as they digested long transcripts transcribed from clones and full-length mRNA from total retinal RNA extracts in vitro. At increasing intervals after subretinal injection with either AAV ribozyme, a 30% to 90% reduction in a- and b-wave amplitudes was observed compared with those in contralateral control eyes that were not injected. Retinal tissue analysis showed that loss of the photoreceptor cells and PDEγ mRNA and protein paralleled the ERG results.

CONCLUSIONS. Ribozyme-mediated somatic knockdown of wild-type PDEγ mRNA in vivo can efficiently reduce the target RNA leading to a loss in rod photoreceptors and in rod-mediated ERG amplitudes, thus generating an animal model of retinal degeneration resembling human RP in an essentially normal adult retina. This vector ribozyme technique should be applicable to other genes associated with RP and perhaps also to mRNAs of phototransduction genes not yet associated with RP. Application of this approach may be age and species independent. (*Invest Ophthalmol Vis Sci.* 2005;46: 3836–3844) DOI:10.1167/iovs.04-1283

Rod photoreceptor cyclic GMP-phosphodiesterase (cGMP-PDE) is one of the key enzymes of the visual phototransduction cascade in the vertebrate retina.[1] The enzyme is composed of α- and β-catalytic subunits (PDEαβ) and two copies of the inhibitory γ-subunit (PDEγ).[2] In phototransduction signaling, PDEγ is a multifunctional protein that may interact either directly with both the catalytic subunits (PDEαβ) and or with the α-subunit of transducin (Tα).[3,4] Photoactivation of the visual pigment rhodopsin leads to activation of the G-protein, transducin (Tα), which, in turn, proceeds to stimulate cGMP-PDE. The activated α-subunit of transducin (Tα) is then believed to interact with the membrane-associated rod PDE holoenzyme (subunit stoichiometry, $\alpha\beta\gamma_2$) displacing the inhibitory PDEγ subunits from the active sites of the catalytic heterodimer PDEαβ. The enhanced hydrolytic activity of activated PDE rapidly reduces cytoplasmic cGMP levels, leading to closure of cGMP-gated cation channels and hyperpolarization of rod and cone cells.[5–7]

A defect in any PDE subunit may alter the activity of the enzyme, leading to aberrations in the visual phototransduction. Mutations in the PDEβ subunit gene cause inherited retinal diseases associated with retinitis pigmentosa (RP) in humans[8] as well as in *rd* mice[9–11] and Irish Setter dogs.[12] Mutations in the PDEα[13] and PDEγ[14,15] genes can also produce RP in human and RP-like symptoms in mice.

The human gene for PDEγ maps to a distal region of the long arm of chromosome 17 (17q25), and no inherited retinal degenerations have yet been mapped to this gene. Nevertheless, several mutations in the murine PDEγ gene (*Pdeg^{tm}*, Del 7C, Y84G, and W70A) [15–18] have been studied in the past decade. Mutations in PDEγ (PDEγ knockout *Pdeg^{tm}* mice) result in rapid retinal degeneration and represent one of the more aggressive forms of human RP. In homozygous mutant mice, reduced PDE activity was observed; the PDEαβ dimer was formed but lacked hydrolytic activity. The *Pdeg^{tm}* mice may suffer retinal degeneration through a mechanism similar to that in the *rd1* mouse, in that the high cGMP concentration may keep cGMP-gated cationic channels continuously open and lead to an excessive load on rod photoreceptors, resulting in degeneration. The generation of a more extensive allelic series of mutant mice (Del 7C, Y84G, and W70A) further demonstrated the consequences of continuous excitation on photoreceptor development and survival: some of these mice did not respond to light, possibly resulting from a stationary rod dysfunction but without degeneration. Thus, these animals provide important information about mechanisms of light adaptation in response to constitutive signaling and allow the study of retinal degeneration caused by deficient PDEγ.[14–18]
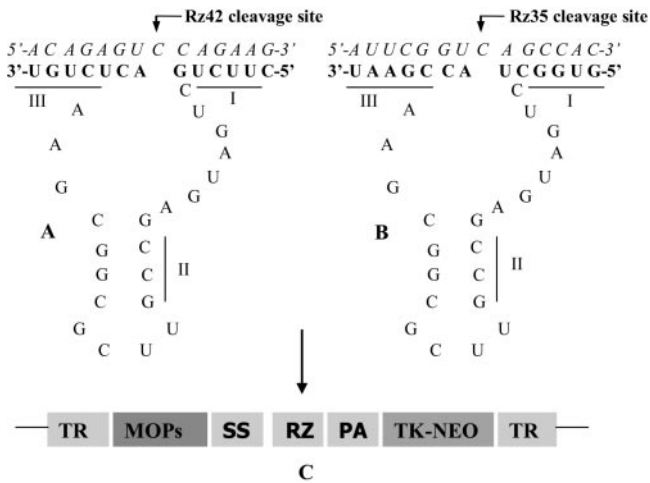
FIGURE 1. Secondary structure of hammerhead ribozymes. *Italic letters*: the target RNA sequence of the rod PDEγ mRNA of the wild-type mice; *nonitalic letters*: the ribozyme sequence. *Roman numerals* label the helices. The hammerhead ribozyme HRz42 cleaves at position −42 (**A**) and HRz35 cleaves at position 35 (**B**) of the rod PDEγ gene. (**C**) The recombinant AAV cassette of the pTR plasmid used to produce rAAV-MOPS-RZ. TR, inverted terminal repeats; MOPs, murine rod opsin promoter (472 bp); SS, splice donor/acceptor site; PA, polyadenylation termination signal; TK-Neo, thymidine kinase promoter driving expression of the G418- resistance gene.

The development of viable retinal gene therapy regimens is critically dependent on the availability of suitable animal models.[19] In an attempt to generate an animal model of retinal degeneration, we used an rAAV-ribozyme–mediated approach to knockdown of the rod PDEγ mRNA in wild-type mice. Hammerhead and hairpin ribozymes possess the dual properties of RNA sequence-specific recognition and site-specific cleavage of target RNA molecules. These properties provide powerful tools for studies requiring inhibition of gene-function. However, the hammerhead ribozyme has been used more commonly, because it imposes few limitations on target RNA molecules and it is small (35 nucleotides [nt]) and highly reactive.[20–22] The choice of ribozyme delivery vehicle was based on our previous experience using adenoassociated virus (AAV) to deliver ribozymes as therapy in animal models of dominant inherited retinal diseases.[23–25] This AAV ribozyme approach, in theory, permits somatic knockdown of genes in normal adult tissue, thus avoiding problems commonly associated with transgenic or germ-line knockout animal, including embryonic lethality or experimental inaccessibility due to early developmental expression. This technique also avoids the time and expense of creating transgenic animals. In this study, we tested the idea that AAV ribozyme in vivo somatic to knockdown of PDEγ mRNA in wild-type mice would lead to defects in rod function and viability, thus mimicking those in the knockout mouse.[15]

MATERIALS AND METHODS

Cloning of Ribozymes and Targets

Two hammerhead ribozymes were designed to target and cleave the γ-subunit of the rod cGMP-PDEγ mRNA in the retina of wild-type mice. The total cDNA sequence of the mouse rod PDEγ gene is 482 nt, of which 261 nt comprise the coding region, 121 nt are in the 5′-untranslated region and 100 nt are in the 3′-untranslated region.[26] One ribozyme was designed to target PDEγ mRNA at position −42 of the 5′-untranslated region (Rz42) and another targeting position +35 in the coding region (Rz35; Fig. 1).

Ribozyme coding sequences were generated by extension of two overlapping synthetic DNA oligonucleotides flanked by the *Eco*RI and *Mlu*I restriction sites. These oligonucleotides were annealed by heating at 94°C for 2 minutes in 20 mM Tris-HCl (pH 7.5) and 50 mM NaCl, then incubated at 55°C for 15 minutes and shifted to ice for another 5 minutes. The annealed oligonucleotides were ethanol precipitated and resuspended in dH₂O and the single-stranded regions filled with 10 units of the large fragment of DNA polymerase I (Invitrogen, Carlsbad, CA) in 1 mM dNTPs, and reaction buffer 3 (Invitrogen) at 37°C for 1 hour. The fully duplexed fragments were digested and ligated into the plasmid pHC[27] at the *Eco*RI and *Mlu*I restriction sites downstream of a T7 RNA polymerase promoter sequence. Ligated plasmids were transformed into competent *Escherichia coli* DH5-α cells by heat shock at 42°C for 90 seconds. Clones were screened by restriction digestion and verified by sequencing.

Three different targets—short synthetic RNA oligomers, cloned longer synthetic transcripts, and full-length in vivo RNA—were designed to test ribozymes at different levels. The short synthetic RNA oligomer targets (14 nt) were ordered directly from Dharmacon (Lafayette, CO). These RNA oligonucleotides are protected on their 2′ residues and must be deblocked by mild acid treatment before use. The longer cloned target (114 nt), which covers both cleavage sequences of ribozyme HRz35 and HRz42 in the wild-type mouse PDEγ sequence, was constructed by cloning a fragment of the cDNA in the pHC plasmid described earlier. The full-length RNA target was contained in total retinal RNA by extraction from whole retina of treated and untreated eyes, according to the manufacturer's instructions (TRIzol reagent; Invitrogen).

In Vitro Transcription

For in vitro transcription, plasmids containing ribozyme sequences or cloned targets were linearized with *Mlu*I, phenol extracted, and ethanol precipitated. Transcripts were generated with T7 RNA polymerase and labeled by incorporation of [α-³²P] UTP (ICN, Costa Mesa, CA) using the protocol of Grodberg and Dunn.[28] Transcription products were filtered through a spin column (Sephadex G-25; Roche Diagnostics, Indianapolis, IN), extracted with phenol-chloroform-isoamyl alcohol (25:24:1) twice and chloroform once and then ethanol precipitated with 1 μL glycogen or dextran blue carrier, washed with 70% ethanol, and resuspended in diethylpyrocarbonate (DEPC)-treated water. For determining the specific radioactivity of transcription products, 1 or 2 μL of samples were spotted on glass fiber filters and analyzed by scintillation counting. Finally, the concentration of ribozymes or targets was calculated by the specific radioactivity.[29]

Ribozyme Cleavage Reactions

Ribozyme cleavage reactions were performed in a volume of 10 μL containing 50 nM target RNA, 10 nM ribozyme, 20 mM MgCl₂, and 40 mM Tris-HCl (pH 7.5) and incubated at 37°C for the indicated times (see Fig. 2A). Cleavage reactions were stopped by addition of 50 mM EDTA, 10 M urea, 0.02% bromophenol blue, and 0.02% xylene cyanol. Cleavage products were analyzed by electrophoresis on 15% (wt/vol) polyacrylamide denaturing gels (8 M urea) in Tris-boric acid-EDTA (TBE) buffer and scanned (Storm PhosphorImager; GE Healthcare, Piscataway, NJ). The fraction cleaved was calculated from the ratio of radioactivity in the cleavage product to the sum of the radioactivity in the cleavage product plus the reaction target in the same lane of the gel. The observed reaction velocity is given as the fraction cleaved per minute.[29]

Kinetic Analysis

Time-course reactions were performed in a volume of 20 μL containing a concentration of ribozyme at least 10-fold in excess of target RNA, usually 20 to 100 nM ribozyme with 2 to 10 nM of RNA substrate. Other reaction conditions are as described in the cleavage reaction. For multiple turnover kinetics analysis, reactions were performed with 2 to 5 nM ribozyme with increasing concentrations of substrates, from 20

to 500 nM using [α-^{32}P]-ATP end-labeled RNA targets, under the conditions described earlier for short intervals. The reaction products were analyzed as described earlier. The kinetic constants K_m and K_{cat} were determined from Eadie-Hofstee plots.[30]

rAAV-Ribozyme Constructs

Recombinant AAV constructs were based on the pTR-UF2 vector.[31,32] Each ribozyme gene as derived from the pHC plasmid as described earlier was inserted into the *Not*I sites of pTR-UF2, replacing the GFP gene and replacing the CMV promoter with a 472-bp proximal murine rod opsin promoter (mOp472) to drive ribozyme gene expression specifically and efficiently in rodent photoreceptors (PR) cells[31] (Fig. 1C). The resultant pTR-MOPS vectors with ribozyme genes were package into serotype 5 rAAV capsids by standard procedures.[31] The constitutive transport element was placed downstream of the ribozyme cassette to facilitate RNA transport and stability.[33] Vector-ribozyme genome–containing particle titers were determined by quantitative competitive PCR (QC-PCR) for the *neo*[r] gene.

Subretinal Vector Injection

All animal procedures used were in agreement with the NIH Guide for the Care and Use of Laboratory Animals, the ARVO Statement for the Use of Animals in Ophthalmic and Vision Research, and institutional guidelines and were approved by the University of Florida Institutional Animal Care and Use Committee. All C57BL/6J mice were purchased from Jackson Laboratories (Bar Harbor, MA).

Three-week old wild-type mice (C57BL/6J) from The Jackson Laboratory were used. Animals were anesthetized by ketamine-xylazine injection, eyes were dilated (2.5% phenylephrine and 0.5% tropicamide), and a local anesthetic (proparacaine HCl) was applied. Injections (1 μL) were made into the right eye with blunt 33-gauge needles through an opening in the pars plana, delivering the rAAV-ribozyme suspension into the superior subretinal space. Control injections of rAAV-inactive ribozyme were made in the partner control eye, or the eye was left untreated. Injections were performed with an operating microscope, and the subretinal location of the injected volume was confirmed by ophthalmoscopy.[34]

ERG Analysis

The injected mice were dark-adapted overnight and anesthetized with intramuscular injection of xylene (13 mg/kg) and ketamine (87 mg/kg) under dim red light. Full-field scotopic ERGs were measured with 10-μs flashes of white light and responses were recorded with a visual electrodiagnostic system (UTAS-E 2000; LKC Technologies, Gaithersburg, MD). Stimuli were presented at intensities of 0.02, 0.18, and 2.68 cd-s/m^2 at 10-, 20-, and 30-second intervals, respectively. Five responses were averaged at each intensity. The a-waves were measured from the baseline to the peak in the cornea-negative direction, and b-waves were measured from the cornea-negative peak to the major cornea-positive peak. For quantitative comparison of differences between eyes of one mouse, values from each of the stimulus intensities were averaged for each eye.[25,34] For determining the significance of differences between treated eyes (usually right-eye) and partner control eyes (usually left-eye), statistical analyses were performed on computer with a two-sample Student's *t*-tests assuming equal variances, two-sample assuming unequal variances, and paired two-sample for means (Excel; Microsoft, Redmond, WA). The same statistical analyses were used in RT-PCR or other data analyses in the study.

Isolation of RNA and RT-PCR for Detecting PDEγ mRNA In Vitro and In Vivo

Total RNA was isolated from the retinas of wild-type mice for assaying cleavage of full-length rod PDEγ mRNA in vitro and from the treated mice to measure a reduction in levels of the rod PDEγ mRNA in vivo. For measurement of cleavage in ribozyme-treated mice, RNA was extracted 3 weeks after subretinal injection with rAAV-ribozymes. RNA

was isolated from the retinas according to manufacturer's protocol (TRIzol reagent; Invitrogen). After the ethanol precipitation step in the extraction procedure, the RNA samples were treated with RNase-free DNase (Qiagen, Valencia, CA) to remove genomic DNA contamination. After this, the RNA was repurified using a clean-up protocol (RNeasy Mini Kit; Qiagen) according to the manufacturer's instructions. Finally, the RNA was eluted into RNase-free H$_2$O to obtain approximately 0.5 μg/μL and stored in small aliquots at $-80°$C. The RNA concentration was determined spectrophotometrically at 260 and 280 nm, and its integrity was verified by the electrophoresis in formaldehyde agarose gels (1.2%). Each RNA sample came from a separate eye (no pooling).

Even though the ribozymes Rz35 and Rz42 can cleave an RNA substrate 114 nt in length, it is important to test its activity on the full-length PDEγ mRNA, because of the possibility of additional secondary structure in full-length mRNA. For this purpose, total retinal RNA was extracted from the C57BL wild-type mice as described earlier. Ribozyme cleavage reactions in vitro were performed in duplicate by using a volume of 10 μL containing 1 μg total retinal RNA, 10 nM ribozyme (three different treatments: Rz42, Rz35, and no Rz), 20 mM MgCl$_2$, 40 mM Tris-HCl (pH 7.5), and 0.1μL RNase inhibitor (Promega, Madison, WI) and incubated at 37°C for the indicated times (see Fig. 2A). Two microliters of the cleavage reactions for each treatment were obtained at each time point and analyzed by RT-PCR.

Reverse transcription (RT) reactions were accomplished with reverse transcriptase and olig-dT or reverse primer by using the a first-strand cDNA synthesis kit according to the manufacturer's protocol (GE Healthcare). For each RT reaction, 2 μL of the cleavage reaction RNA (1 μg) was added to 1 μL of reverse primer (10 picomoles, 5'-CAAGGGCAGA TGACGGTGA-3') and heated to 65°C for 5 minutes. To this, 8 μL of a mix containing buffer and enzyme (supplied with kit) was added (total RT reaction: 10 μL). This was incubated for 1 hour at 37°C followed by a 90°C incubation for 5 minutes, to inactivate the reverse transcriptase.

The RT reaction was used as a template for the polymerase chain reaction (PCR). PCR primers were designed to cover the cleavage sites for the two ribozymes Rz42 and Rz35 within a PDEγ gene and were synthesized by Invitrogen (forward primer: 5'-TCTGTCCAGT GCTT-GCCTGC-3'; reverse primer: 5'-CAAGGGCAGA TGACGGTGAT-3'). Additional primers were designed to amplify β-actin as the internal control (forward primer: 5'-GTTTGAGACC TTCAACACCC-3'; reverse primer: 5'-TACTCCTGCT TGCTGATCCA-3'). The linear range of the amplification of the PDEγ RT-PCR product was determined by using a PCR mix containing 10 μL RT product, 200 μM dNTPs, 1 mM MgCl$_2$, 0.2 μM PDEγ, 0.1 μM β-actin oligonucleotides (primers), 1$\times$ *Taq* DNA polymerase buffer, 2 units *Taq* DNA polymerase (Invitrogen), and 0.5 μCi/50 μL [α^{32}P]-dATP (ICN). The PCR mix (total PCR reaction, 50 μL) was separated into 0.2-mL tubes, and amplification was performed in the following program on a thermocycler (model T3; Bio-Metra, Göttingen, Germany): 95°C for 5 minutes; 26 cycles at 94°C for 30 seconds, 60°C for 30 seconds, and 72°C for 45 seconds; and a final extension of 72°C for 10 minutes; followed by a pause at 4°C. Samples were removed at the exponential phase in preliminary experiments. Preliminary experiments had shown that the exponential phase of both PDEγ and β-actin was at cycle 26.

For each PCR sample, 5 μL was removed and 2 μL of dye mix was added. The samples were loaded onto a 4% polyacrylamide 8-M urea gel. Dried gels were analyzed on the phosphorescence imager (Storm PhosphorImager; GE Healthcare) or imaged by autoradiography with x-ray film to determine the linear range of amplification. The fraction cleaved was calculated from the ratio of radioactivity in the PDEγ band to the β-actin band for each lane.

For detecting a reduction in levels of the rod PDEγ mRNA, the right eyes of wild-type mice were subretinally injected in vivo with rAAV ribozyme and the fellow eyes were left untreated as a partner control, at postnatal day (P)21. Three weeks after subretinal injection, the total RNA was extracted and analyzed by RT-PCR, as described earlier.
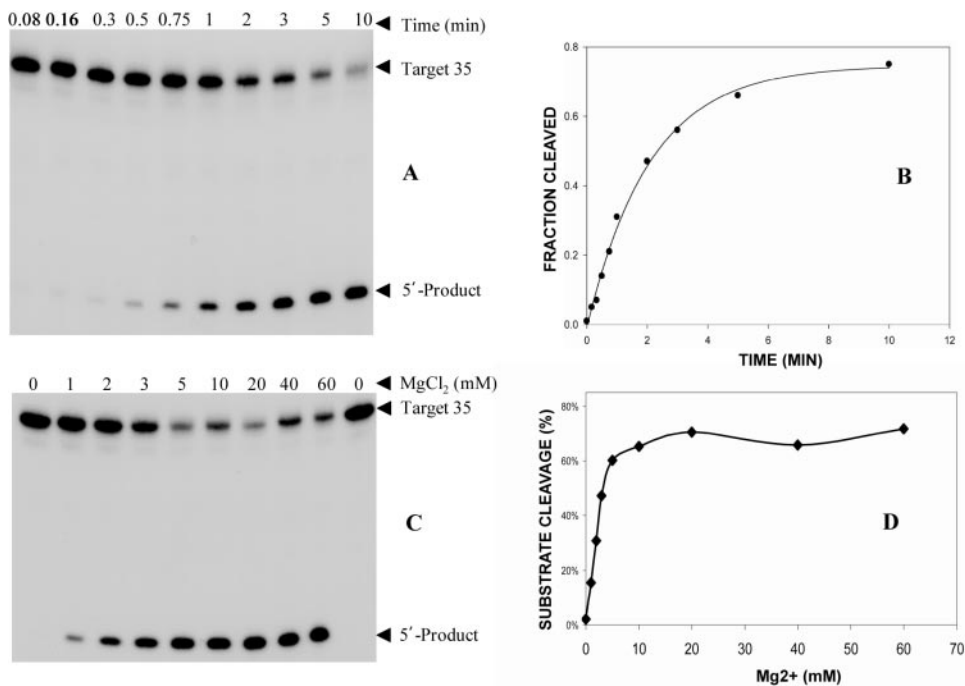
FIGURE 2. Cleavage properties of HRz35. (**A**) Autoradiogram of the HRz35 cleavage reaction with increasing time. The samples were incubated in 20 mM $MgCl_2$ and 40 mM Tris-HCl (pH 7.5) at 37°C. (**B**) The amount of cleavage product formed by HRz35 plotted against time. The substrate was a 14-nt end-labeled RNA. (**C**) Magnesium dependence. Ribozyme and target were incubated for 15 minutes at 37°C in increasing concentrations of $MgCl_2$. Shown is a representative autoradiogram of the reaction samples. (**D**) Magnesium titration of HRz35 cleavage of synthetic RNA targets (14 nt).

Western Immunoblot Assay

At P21, the right eyes of mice were injected with active ribozyme, and left eyes remained untreated. Three weeks after subretinal injection, total protein was extracted (TRIzol Reagent; Invitrogen) according to the manufacturer's protocol. The total protein concentration was determined, and the equivalence of protein extraction from left and right eyes was confirmed with Coomassie brilliant blue staining (Bio-Rad, Hercules, CA) after SDS-polyacrylamide gel electrophoresis. Total protein (20 μg) was separated on an 18% SDS-polyacrylamide gel and electrotransferred (Trans-Blot Semi-Dry; Bio-Rad) to nitrocellulose transfer membranes. Membranes were probed with rabbit anti-PDEγ antibody (a gift of Theodore Wensel, Baylor College of Medicine, Houston, TX) and with arrestin antibody (a gift of W. Clay Smith, University of Florida, Gainesville, FL). Primary antibodies were diluted 1:1,000 and blots were developed with anti-rabbit IgG conjugated with horseradish peroxidase (HRP; Promega) secondary antibody (diluted 1:10,000). Protein bands were visualized with chemiluminescence detection reagent according to the manufacturer's protocol (ECL Plus; GE Healthcare). Membranes were exposed to autoradiograph film (Hyperfilm ECL film; GE Healthcare) for 5 to 30 seconds.

Retinal Tissue Analysis

Treated mice were euthanatized by an overdose of ketamine and xylazine and were immediately perfused intracardially with a mixture of mixed aldehydes (2% paraformaldehyde and 2.5% glutaraldehyde). Eyes were immediately enucleated, and the cornea, lens, and vitreous of each eye removed. The posterior eye cup was then placed in the primary fixative (4% paraformaldehyde) for 4 hours or overnight at 4°C. The tissues were dehydrated and embedded in epoxy resin, and 1-μm-thick histologic sections were made along the vertical meridian. The thickness of the rod outer nuclear layer (ONL) was determined as the average number of rows of photoreceptor nuclei in four nonadjacent sections at four positions in each section.[35]

RESULTS

Cleavage Time Course

Two hammerhead ribozymes were engineered to digest wild-type PDEγ mRNA. To study cleavage activities on a variety of substrates, three different targets (short synthetic, cloned longer and full-length RNA) were used. Initially, two short synthetic RNA targets (14 nt) containing the cleavage site at positions +35 and −42 were used to determine the reaction time course, the magnesium optima, and the kinetic behavior of the ribozymes. For the cleavage time course, ribozymes HRz35 and HRz42 were incubated with excess substrate at physiologic temperature but at high magnesium concentrations (20 mM) to promote ribozyme folding. The cleavage products increased significantly with time. Approximately 80% (Rz35) and 75% (Rz42) of the targets were cleaved after a 10-minute incubation (Figs. 2A, 2B) and almost 100% of each target was digested by 20 minutes (data not shown).

Magnesium Dependence of the Cleavage Reaction

Magnesium is required for correct folding of hammerhead ribozymes and possibly for hydrolysis of the phosphodiester bond.[36,37] Ribozyme activity is therefore typically quite sensitive to the level of magnesium in the reaction. The magnesium dependence of HRz35 and HRz42 were determined using oligonucleotide targets under our standard buffer conditions (Figs. 2C, 2D). The activity of both ribozymes increased with the increase in magnesium concentration, reaching a plateau near 8 mM, with no further increase up to 60 mM. It is important to note that both ribozymes are active at magnesium concentrations of 2 mM, indicating that cleavage should occur efficiently under physiological conditions.

Kinetic Analysis

To determine the cleavage efficiencies of ribozymes pHRz42 and pHRz35 against synthetic targets (14 nt), multiple turnover cleavage reactions were performed under conditions of excess substrate with the ribozyme concentration kept constant. The kinetic parameters K_m and K_{cat} determined from this analysis for the two ribozymes are shown in Table 1. Whereas the K_m values are almost identical, reflecting similar binding affinities for their respective target sites, there was an almost threefold difference in K_{cat} between HRz35 and HRz42, indicating a difference in overall enzymatic turnover. The physiological

TABLE 1. Ribozyme Properties

Ribozymes	K_{cat} (min)	K_m (nM)	K_{cat}/K_m (M/min)	Mg^{+2} Optimum
pHRz35	0.48	980	4.9×10^5	8 mM
pHRz42	0.17	971	1.8×10^5	8 mM

activity of enzymes is determined best by the K_{cat}/K_m ratio, because the ratio accounts for diffusion as well as affinity and chemistry. The ribozymes pHRz35 and pHRz42 had K_{cat}/K_m of 4.9×10^5 and 1.8×10^5, respectively, indicating that the ribozyme pHRz35 is more active than that pHRz42. However, both ribozymes are in the range that we have used for successful experiments in cells and animals.[23]

Cleavage of Longer Target mRNAs

Because RNA secondary structures may block access of a ribozyme to its binding–cleavage site, we also tested the PDEγ ribozymes on a transcript of 114 nt containing cleavage sites for both HRz35 and HRz42. Most stable secondary structures such as internal stem loops form locally, so that an RNA of this size should reflect the accessibility of the ribozyme target sites in the full-length mRNA (482 nt). The cleavage reactions were incubated as described for 2 hours, and the products were resolved on denaturing polyacrylamide gels (Fig. 3). Such long targets are not suitable for kinetic analysis, since the rate-limiting step in such reactions is not the cleavage reaction. However, this experiment indicates that both ribozyme target sites in the native substrate are accessible to cleavage.

Cleavage of Full-Length mRNA Targets

Although ribozymes HRz42 and HRz35 can cleave synthetic RNA oligomers of 14 nt and a RNA target of 114 nt, it is useful to confirm cleavage activity on the full-length mRNA target because of the possibility that alternative RNA conformations could obscure the target sites. If the ribozymes can cleave the full-length mRNA within the context of total retinal RNA in vitro, it is likely that they will be able to do so within photoreceptor cells as well, because nuclear proteins such as hnRNP.A protein have been shown to facilitate RNA digestion by ribozymes.[38] Therefore, total retinal RNA extracts from wild-type mice were used as full-length mRNA target substrates in standard ribozyme reactions (Fig. 4). In this case, RT-PCR
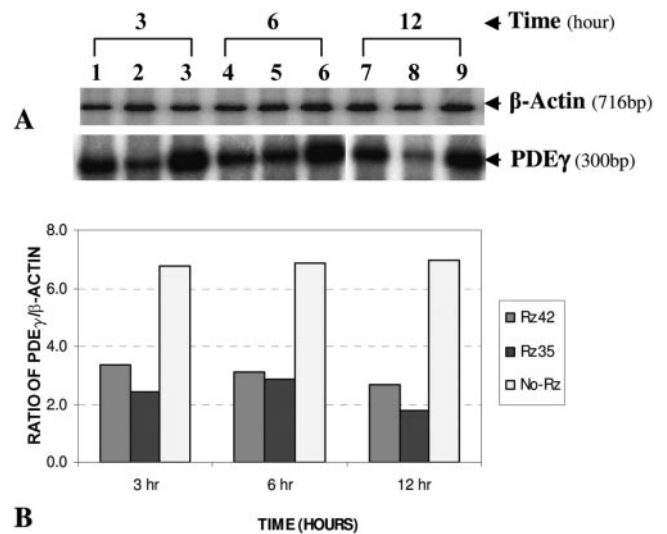
FIGURE 4. The cleavage reaction from ribozymes HRz42 and HRz35 against the rod full-length PDEγ mRNA in vitro. (A) Autoradiogram of RT-PCR products after 3, 6, and 12 hours of incubation. *Lanes 1, 4, and 7*: HRzs42; *lanes 2, 5, and 8*: HRz35; *lanes 3, 6, and 9*: the control (No-Rz) samples incubated for the same times without ribozymes. (B) Quantification of RT-PCR products. The fraction cleaved (ratio of PDEγ/β-actin) was calculated from the ratio of radioactivity in the PDEγ intensities to the β-actin intensities for each lane.

was used to detect the activity of the ribozyme against full-length mRNA target. Cleaved targets resulting from addition of either ribozyme to the total retinal RNA should reduce the level of PDEγ-specific RT-PCR product compared with the total retinal RNA without ribozyme. Relative to control samples incubated without ribozyme, the amount of target digested by the ribozymes HRz42 and HRz35 was 51% and 65% at 3 hours, 55% and 58% at 6 hours, 61% and 74% at 12 hours, respectively.

PDEγ Ribozymes and the Response to Light

For in vivo experiments, ribozymes HRz35 and HRz42 were packaged in an AAV vector downstream of a proximal MOPS promoter (Fig. 1) and subretinally injected into the eyes of 3-week-old mice. The titer of AAV ribozyme vector particles for HRz35 and HRz42 were 8×10^{13} and 1.6×10^{13} mL, respec-
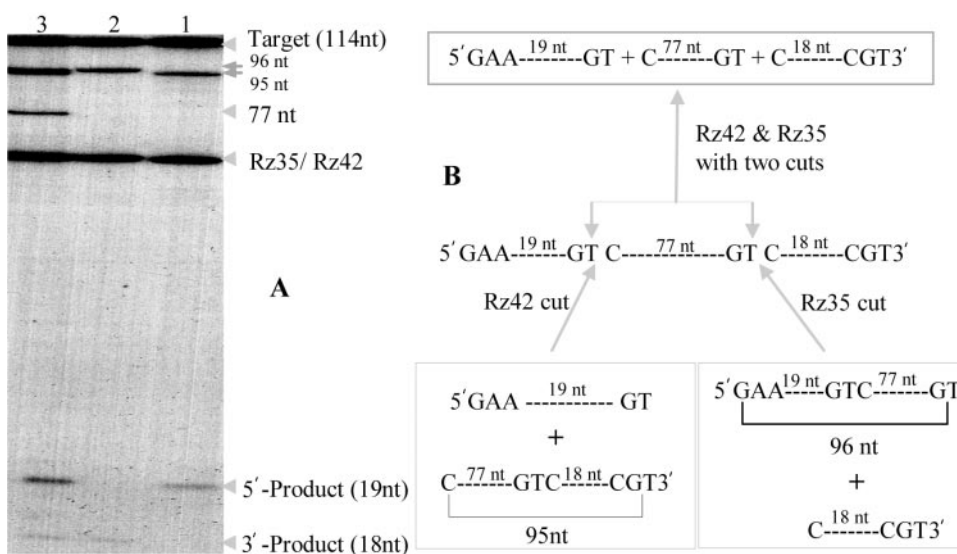
FIGURE 3. Cleavage reaction of ribozymes pHRz35 and pHRz42 using cloned RNA targets. (A) Autoradiogram of pHRz35 and pHRz42 reactions (alone or together) with the internally labeled cloned target transcript. *Lane 1*: HRz42 alone; *lane 2*: HRz35 alone; *lane 3*: HRz35 and HRz42 together. Samples were separated on a 10% polyacrylamide, 8-M urea gel, and visualized by autoradiography. (B) Schematic cleavage of site specificity for both ribozymes HRz35 and HRz42. The cloned target was 114 nt. If ribozyme pHRz35 produced a single cut, cleavage products of 96 and 18 nt were expected. If ribozyme pHRz42 produced a single cut, 19- and 95-nt products are expected. If pHRz35 and pHRz42 were used together, fragments of 19, 77, and 18 nt with 96 and 18 nt, and 19 and 95 nt (two single-cutting products) were expected.
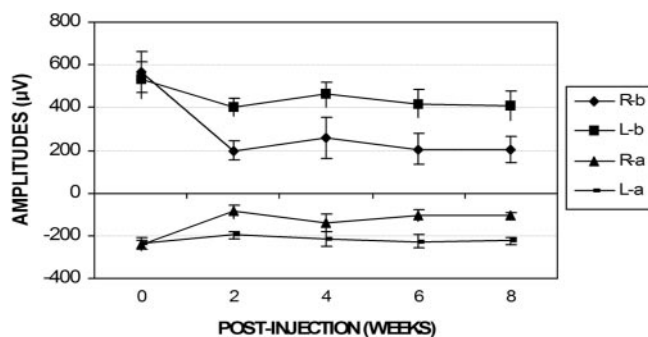
FIGURE 5. The ERG time course at 2 to 8 weeks after injection. Scotopic full-field ERGs were measured in dark-adapted mice in response to flashes of intense white light (0.18 cd-s/m^2). Measurements were taken at 2, 4, 6, and 8 weeks after injection. The rAAV-Rz was injected into the right eye, and the left eye remained untreated. The average of a- and b-wave amplitude maxima is plotted ($n = 10$). Ra, Rb: stand for the a- and b-waves of the right eye; La, Lb: a- and b-waves for the left eye.

tively. One microliter of AAV-ribozyme was injected into the right eyes of C57Bl/6 mice. Recombinant AAV expressing inactive ribozyme was injected into the subretinal space of right eyes of a second cohort of animals, and the left eyes were not injected. In a third group of mice, neither eye was injected. Electroretinography (ERG), morphology, and RT-PCR were then used to assay the effects of these treatments as a function of time after treatment.

ERGs were recorded before injection and at 2, 4, 6, and 8 weeks after injection. The change in ERG amplitudes after injection with HRz35 is shown in Figure 5. Relative to the noninjected contralateral eyes, average ERG a- and b-wave amplitudes were reduced by more than 50% at 2 weeks after injection and remained at approximately this level for the duration of the experiment (8 weeks). We compared the effect of inactive and active ribozymes in detail at the 6-week time point (Fig. 6). Whereas there was a statistically significant difference ($P < 0.01$) in maximum a- and b-wave amplitudes between the injected and noninjected eyes of animals treated with the active ribozyme HRz35 (Rz), the difference between injected and noninjected eyes of mice treated with inactive HRz35 (InaRz) was not significant (Fig. 6A). In addition, there was a significant difference ($P < 0.01$) in the ERG a- and b-wave maximum amplitude ratios (right eye to left eye) between mice treated with the active ribozyme and those treated with inactive ribozyme or untreated, but there was no significant difference between those treated with inactive ribozyme and untreated (Fig. 6B).

PDEγ Ribozymes and the Death of Photoreceptor Cells

Once the ERG analysis had indicated that the functional retinal loss had become stationary, the mice were killed, the eyes enucleated, and the retinas prepared for histology.

The retinas of rAAV-ribozyme knockdown mice were examined histologically at 6 weeks after injection. Light microscopic analysis revealed that in some animals most of retinal outer segments from the injected right eyes were lost and the ONLs were down to one to three layers, but the inner nuclear layer (INL) and ganglion cell layer (GCL) appeared to be unaffected compared with the control left eyes (Fig. 7). When we organized the ERG ratios and histology data, we found that the thinning of the ONL paralleled the ERG decrement. If the ERG decrease was <30%, the ONL exhibited an average of 10 to 12 layers of nuclei. If the ERG loss was from 31% to 50%, seven to

nine layers of nuclei were observed, ERG reductions of 51% and 70% were found in retina with an ONL containing four to six layers, and ERG amplitudes reduced by 71% to 90% reflected two to three layers in the ONL (Table 2).

To determine whether the reduction in light response and in photoreceptor survival was associated with a loss in PDEγ mRNA and protein levels in vivo, the PDEγ mRNA and protein were detected by RT-PCR analysis and Western immunoblot assay for the retinal total RNA and protein, respectively, from AAV-ribozyme–treated right eyes and noninjected control left eyes. The reduction in levels of the rod PDEγ mRNA was 40% to 80% (Fig. 8). The result of a Western immunoblot assay showed that, in rAAV-ribozyme–injected eyes, there was a three- to fivefold reduction in levels of the rod PDEγ protein compared with the untreated control left eyes (Fig. 9). In this experiment, we used inactive ribozyme as a control to distinguish knockdown due to the catalytic activity of the ribozyme. The variability in these results most likely reflects an uncertainty in the precise volume of vector delivered subretinally from mouse to mouse. These measurements were made at 3 weeks after injection, before substantial loss of photoreceptors had occurred; therefore, loss of PDEγ is not caused by loss of cells. (Note that arrestin levels are not diminished in treated eyes at this stage.) Rather, reduction in the level of the rod PDEγ protein in infected cells is likely to be the cause of the
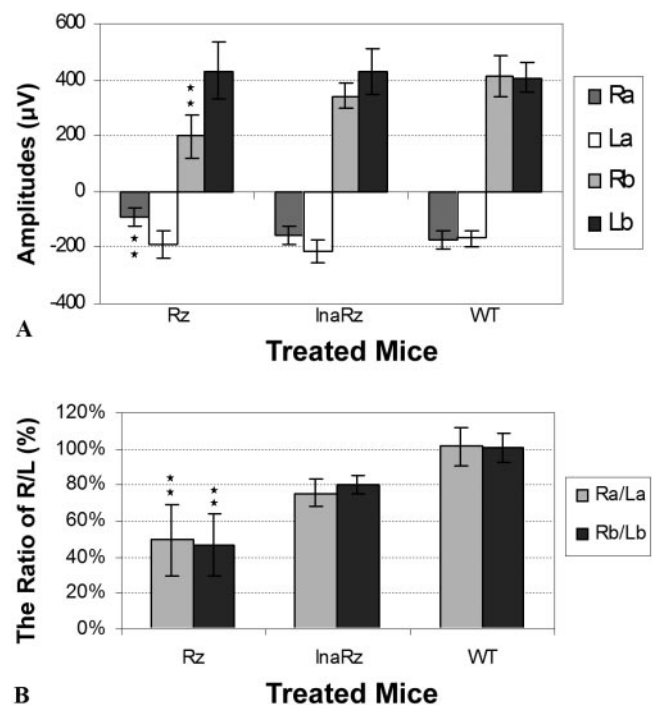

FIGURE 6. Comparison of a- and b-wave maximum amplitudes of rAAV-Rz, rAAV-Ina-Rz, and noninjected mice. Scotopic full-field ERGs were measured at 6 weeks after injection in dark-adapted mice in response to flashes of intense white light (0.18 cd-s/m^2). The rAAV-Rz or rAAV-Ina-Rz was injected into right eyes, and left eyes were not injected. One group of animals was not injected in either eye. **(A)** Average maximum a- and b-wave amplitudes after subretinal injections. There is a significant difference ($P < 0.01$) between the right eyes of the rAAV-Rz group ($n = 25$) and the control left eyes of this group, right eyes of the inactive Rz group ($n = 8$; $P < 0.01$), and the noninjected group ($n = 5$; $P < 0.01$). There is no significant difference between the Ina-Rz and NI groups on both a- and b-waves. **(B)** Ratio of right eye and left eye of the maximum a- and b-wave amplitudes after subretinal injection. Again, the difference between Ina-Rz and NI groups is not statistically significant. Groups are as denoted in Figure 5. RZ, ribozyme; Ina-RZ, inactive-ribozyme; WT, wild type (no injection).

FIGURE 7. Loss of photoreceptor cells parallels loss of ERG response. Mice were injected with rAAV-RZ in the right eye only and analyzed at 6 weeks after injection. The results are organized according to the ratio of ERG amplitudes in the right (treated) to left (untreated) eyes. (A) An rAAV-RZ-injected mouse in which the ERG ratio for the right-to-left eye a-wave amplitude was 19% (i.e., an 81% loss) and 22% for the b-wave amplitude (i.e., a 78% loss). The ONL had only one to three nuclear layers, with most of the rod outer (ROS) and inner (RIS) segments lost. (B) An rAAV-Rz-injected mouse in which the ERG ratio is 41% for the a-wave and 43% for the b-wave. The ONL had four to six nuclear layers with somewhat more ROS and RIS remaining. (C) An rAAV-RZ-injected mouse in which the ERG ratio was 56% for the a-wave and 61% for the b-wave. The ONL had seven to nine nuclear layers, with nearly normal ROS and RIS. (D) rAAV-InaRz (inactive ribozyme) injected in the right eye and no injection in the left eye. The ERG ratio was 86% for the a-wave and 81% for the b-wave. The ONL had 10 to 12 layers with normal-appearing ROS and RIS, nearly the same as in noninjected wild-type mice (data not shown). The amplitude of each ERG was 50 μV/div vertically and 10 ms horizontally at three different intensities (0.02, 0.18, and 2.68 cd-s/m^2).
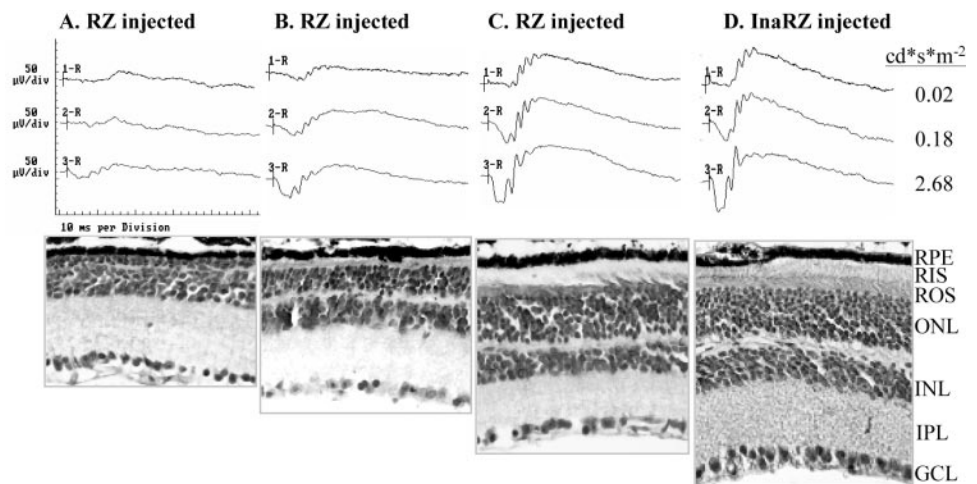
reduced visual response, as measured by the dampened ERG response and the death of photoreceptor cells.

DISCUSSION

The function of rod and cone PDE is to hydrolyze intracellular cGMP on activation of PDE by release of its γ-subunits. Genetic defects leading to changes in cGMP levels are a common cause of retinal disease in animal and human.[39] Somewhat paradoxically, even though PDEβ is a catalytic subunit and PDEγ is an inhibitory subunit, both PDEβ and PDEγ null mice have elevated levels of cGMP, suggesting that loss of either subunit causes PDE instability. To test this hypothesis, we asked whether ribozyme knockdown of a wild-type rod PDEγ mRNA is sufficient to create a retinal phenotype that mimics the loss of rod function and structure that typically accompanies human RP. Toward this end, two hammerhead ribozymes were designed to target the mouse rod γ-subunit of the rod cGMP-PDEγ mRNA and were tested in normal C57BL/6 mice. Both ribozymes were effective at reducing the in vivo level of PDEγ, reducing ERG amplitudes, and diminishing the number of photoreceptor cells remaining in the retina. We conclude that AAV-vectored ribozymes, if properly screened and validated for activity against their intended target, can lead to the phenotypic hallmarks of the corresponding null mutation.

When rAAV-Rz was injected into the right eye but not into the left eye at P21 to P28, the ERG data from rAAV-Rz mice showed a significant loss, ranging from 30% to 90% in both a-

and b-wave amplitudes. The morphology of photoreceptors was also impacted: the ONL ranged from 3 to 11 nuclear layers with almost total loss of the outer and inner segments in the most severely affected eyes. The INL and GCL appeared to be unaffected in treated eyes compared with the contralateral control at 6 weeks after injection.

By comparison, a gene-targeting approach was used to disrupt the mouse rod PDEγ gene. Tsang et al.[15] developed the targeted mutation Pde^{tm1}/Pde^{tm1} KO mice. The corneal electroretinograms of the Pde^{tm1}/Pde^{tm1} mice showed a severely diminished response in both the a- and b-waves with a delay in b-wave implicit time. The decreases in responses were much greater in 8-week-old than in 2-week-old animals. The ERG became almost undetectable after 3 months, and the morphology of Pde^{tm1}/Pde^{tm1} homozygous mutant mice showed the retina had lost the photoreceptor layer (OS, IS, and ONL) completely by 8 weeks of age, but the INL and GCL appear to be unaffected.[15] Thus, from electroretinogram and morphologic data, both rAAV-Rz knockdown mice and Pde^{tm1}/Pde^{tm1} knockout mice are similar and resulted in a very rapid and severe retinal degeneration resembling human RP. Not surprisingly, rAAV-Rz mediated knockdown of the PDEγ gene produced more variable reductions of ERG responses and photoreceptor/ONL loss than did the gene knockout approach, but permitted comparison of disease in one eye to that in a normal eye in the same animal. These different midstatus and internal comparison pairs may permit evaluation of quantitative impact of rod cell loss on ERG amplitudes. Consequently, an AAV-ribozyme–based approach may be useful in evaluating other

TABLE 2. ERG Amplitudes and ONL Thickness after AAV-Ribozyme Treatments

Phenotype	Range of ERG Loss* (%)	P (Relative to Group Above)	Animals (n)	Frequency (%)	Range of ONL Thickness
~Normal	<30	—	5	25	10–12 nuclei
Moderate	31–50	<0.010	5	25	7–9
Strong	51–70	<0.005	7	35	4–6
Extreme	71–90	<0.007	3	15	1–3
Total affected	31–90		15	75	1–9

* Based on b-wave amplitudes at 0 dB (2.68 cd-s/m^2).

genes associated with RP and perhaps also to knock down mRNAs of phototransduction genes not yet associated with RP to determine whether they may, in fact, may be associated with the disease.

Perhaps the largest difference between ribozyme-induced rod cell degeneration and the natural situation in which a missing gene accounts for a disease phenotype is that functional and structural cell loss is not progressive in ribozyme-treated retinas, as seen in genetic RP models. The reason for this difference is that AAV vectors deliver passenger genes to a subset of photoreceptors[31] and, assuming an effective dose in these cells, once they have responded, the remaining cells are normal and do not degenerate. Thus, the stochastic cell death reported in many PR diseases[40] cannot be reproduced. Rather, photoreceptor cell loss is a step function. This means that, the topography of degeneration reflects the topography of vector gene delivery, very unlike the peripheral-to-central progression of RP in both humans and animal models.

A potentially important advantage of this virally delivered ribozyme technology is that it should be relatively independent of the target species, the age of the animal at time of vector treatment, or the target mRNA itself. Although none of these variables has been explicitly tested in this initial study, there seems to be no theoretical barriers to its usefulness in these contexts. Viral delivery methods and dosages have been established in canines and nonhuman primates, making AAV-mediated gene-silencing plausible in larger animals.[41,42]

There are several other implications and potential applications of this technology. First, since animal age at the time of vector administration can be varied, at least in rodents, from any point between midgestation[43] and adulthood, this sort of gene knockdown could be initiated to ask questions related to retinal development. Second, cellular response to the loss of a specific mRNA could be readily assessed. This would allow studies related to how a given retinal cell type responds to the specific gene knockdown to be addressed. Potential targets might include stress gene induction, initiation of apoptosis, and perhaps an even more global gene expression analysis. Such an array analysis could be used to document families of coregulated genes related to the target, and may, for example,
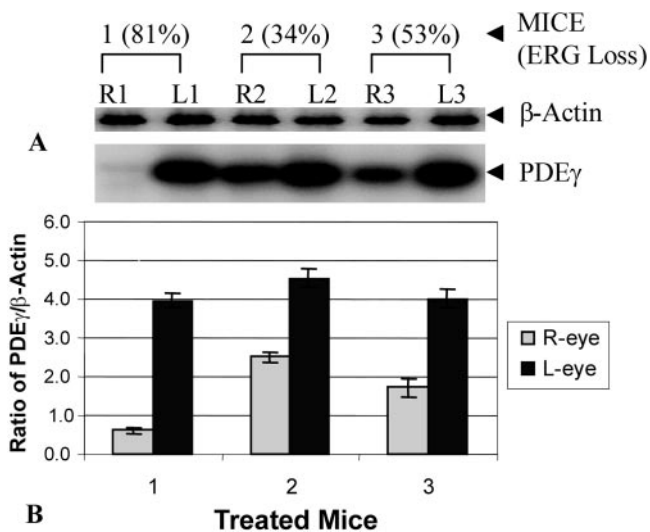

FIGURE 9. Western immunoblot assay for rAAV-Rz[b]-injected mice. *Lanes 1* and *3*: extracts from rAAV-InactRz-injected control left eyes; *lanes 2* and *4*: rAAV-Rz-injected right eyes. Both active ribozyme treated eyes showed reduced levels of PDEγ and unchanged arrestin levels. *Lane 5*: extract from an *rd1* eye, which, as expected, showed no detectible PDEγ or arrestin. *Lane 6*: purified PDEγ protein (5 ng) as a positive control.

reveal currently unrecognized phototransduction genes or known genes with currently unknown relationships to phototransduction. Simply, the response of untargeted phototransduction genes may suggest novel interactions between known phototransduction genes. Third, this approach to somatic gene ablation could aid in identifying currently unrecognized RP-associated genes. Fourth, the potential to knock down both the mutant and wild-type alleles of a dominant acting RP gene and replace both with a gene "hardened" against the ribozyme that still encodes the normal protein[44,45] opens up a more general therapeutic paradigm than direct ribozyme targeting of each mutation in each dominant mutant allele. Because of the allelic heterogeneity of autosomal dominant RP, this RNA replacement approach has significant advantages compared to allele-specific gene-silencing.

References

1. Fung BK-K, Hurley JB, Stryer L. Flow of information in the light-triggered cyclic nucleotide cascade of vision. *Proc Natl Acad Sci USA*. 1981;78:152–156.
2. Deterre P, Bigay J, Forquet F, Robert M, Chabre M. cGMP phosphodiesterase of retinal rods is regulated by two inhibitory subunits. *Proc Natl Acad Sci USA*. 1988;85:2424–2428.
3. Griswold-Prenner I, Tuteja N, Farber DB. G protein-effector coupling: interactions of recombinant inhibitory gamma subunit with transducin and phosphodiesterase. *Biochemistry*. 1989;28: 6145–6150.
4. Whalen M, Bitensky M. Comparison of the phosphodiesterase inhibitory subunit interactions of frog and bovine rod outer segments. *Biochemistry*. 1989;259:13–19.
5. Grunwald ME, Yu WP, Yu HH, Yau KW. Identification of a domain on the beta-subunit of the rod cGMP-gated cation channel that mediates inhibition by calcium-calmodulin. *J Biol Chem*. 1998;273: 9148–9157.
6. Helmreich EJM, Hofmann, KP. Structure and function of proteins in G-protein-coupled signal transfer. *Biochem Biophys Acta*. 1996; 1286:285–322.
7. Pugh EN Jr, Lamb TD. Amplification and kinetics of the activation steps in phototransduction, *Biochim Biophys Acta*. 1993;1141: 111–149.
8. Riess O, Noerremoelle A, Weber B, et al. The search for mutations in the gene for the beta subunit of the cGMP phosphodiesterase (PDEB) in patients with autosomal recessive retinitis pigmentosa. *Am J Hum Genet*. 1992;51:755–762.
9. Bowes C, Li T, Danciger M, Baxter LC, Applebury ML, Farber DB. Retinal degeneration in the rd mouse is caused by a defect in the beta subunit of rod cGMP-phosphodiesterase. *Nature*. 1990;347: 677–680.
10. Bowes C, Li T, Frankel WN, et al. Localization of a retroviral element within the rd gene coding for the beta subunit of cGMP phosphodiesterase. *Proc Natl Acad Sci USA* 1993;90:2955–2959.

FIGURE 8. Reduced levels of the rod PDEγ mRNA after subretinal injection with rAAV-Rz. (**A**) Autoradiogram of RT-PCR products. The numbers 1, 2, and 3 represent three different mice treated with rAAV-ribozyme in their right eyes and untreated in their left eyes. (**B**) The amount of RT-PCR products was measured in duplicate. The reduction in levels (from 40%–80%) of rod PDEγ mRNA was calculated as the ratio of PDEγ product to β-actin product as an internal standard.
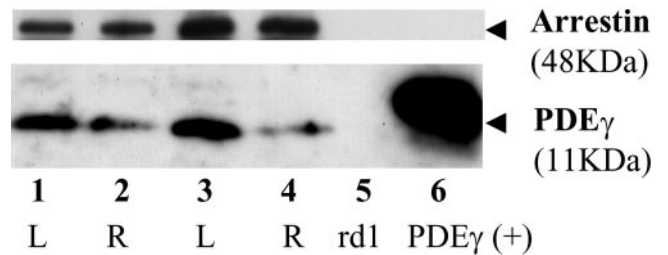
11. Pittler SJ, Baehr W. Identification of a nonsense mutation in the rod photoreceptor cGMP phosphodiesterase beta-subunit gene of the rd mouse. *Proc Natl Acad Sci USA.* 1991;88:8322–8326.

12. Aquirre G, Farber D, Lolley R, et al. Rod-cone dysplasia in Irish setters: a defect in cyclic GMP metabolism in visual cells. *Science.* 1978;201:1133–1134.

13. Huang SH, Pittler SJ, Huang X, Oliveira L, Berson EL, Dryja TP. Autosomal recessive retinitis pigmentosa caused by mutations in the alpha subunit of rod cGMP phosphodiester. *Nat Genet.* 1995;11:468–471.

14. Farber DB, Tsang SH. Stationary night blindness or progressive retinal degeneration in mice carrying different alleles of PDE gamma [review]. *Front Biosci.* 2003;8:S666–S675.

15. Tsang SH, Gouras P, Yamashita CK, et al. Retinal degeneration in mice lacking the gamma subunit of the rod cGMP phosphodiesterase. *Science.* 1996;272:1026–1029.

16. Tsang SH, Burns ME, Calvert PD, et al. Role for the target enzyme in deactivation of photoreceptor G protein in vivo. *Science.* 1998;282:117–121.

17. Tsang SH, Yamashita CK, Doi K, et al. In vivo studies of the gamma subunit of retinal cGMP-phophodiesterase with a substitution of tyrosine-84. *Biochem J.* 2001;353:467–474.

18. Tsang SH, Yamashita CK, Lee WH, et al. The positive role of the carboxyl terminus of the gamma subunit of retinal cGMP-phosphodiesterase in maintaining phosphodiesterase activity in vivo. *Vision Res.* 2002;42:439–445.

19. Hauswirth WW, McInnes RR. Retinal gene therapy 1998: summary of a workshop. *Mol Vis.* 1998;4:11.

20. Hauswirth WW, Lewin AL. Ribozyme uses in retinal gene therapy. *Prog Retinal Eye Res.* 2000;19:689–710.

21. Phylactou LA, Kilpatrick MW, Wood MJ. Ribozymes as therapeutic tools for genetic disease. *Hum Mol Genet.* 1998;7:1649–1653.

22. Vaish NK, Kore AR, Eckstein F. Recent developments in the hammerhead ribozyme field. *Nucleic Acids Res.* 1998;26:5237–5242.

23. Drenser KA, Timmers AM, Hauswirth WW, Lewin AS. Ribozyme-targeted destruction of RNA associated with autosomal-dominant retinitis pigmentosa. *Invest Ophthalmol Vis Sci.* 1998;39:681–689.

24. Hauswirth WW, LaVail MM, Flannery JG, Lewin AS. Ribozyme gene therapy for autosomal dominant retinal disease. *Clin Chem Lab Med.* 2000;38:147–153.

25. Lewin AS, Drenser KA, Hauswirth WW, et al. *Nat Med.* 1998;4:967–971.

26. Tuteja N, Farber DB. Gamma-subunit of mouse retinal cyclic-GMP phosphodiesterase: cDNA and corresponding amino acid sequence. *FEBS Lett.* 1988;232:182–1826.

27. Altschuler M, Tritz R, Hampel AA. Method for generating transcripts with defined 5' and 3' termini by autolytic processing. *Gene.* 1992;122:85–90.

28. Grodberg J, Dunn JJ. Characterization of the genes for the hexagonally arranged surface layer proteins in protein-producing Bacillus brevis 47: complete nucleotide sequence of the middle wall protein gene. *J Bacteriol.* 1988;170:1245–1253.

29. Shaw LC, Whalen PO, Drenser KA, et al. Ribozyme in treatment of inherited retinal disease. *Methods Enzymol.* 2000;316:761–776.

30. DeYoung MB, Siwkowski A, Hampel A. Determination of catalytic parameters for hairpin ribozymes. In: Turner PC, ed. *Ribozyme Protocols.* Totowa, NJ: Humana Press; 1997:209–220.

31. Flannery JG, Zolotukhin S, Vaquero MI, et al. Efficient photoreceptor-targeted gene expression in vivo by recombinant adeno-associated virus. *Proc Natl Acad Sci USA* 1997;94:6916–6921.

32. Zolotukhin S, Potter M, Hauswirth WW, et al. "Humanized" green fluorescent protein cDNA adapted for high-level expression in mammalian cells. *J Virol.* 1996;70:4646–4654.

33. Warashina M, Tomoko K, Yoshio K, Masayuki S, Kazunari TRN. A-protein hybrid ribozymes that efficiently cleave any mRNA independently of the structure of the target RNA. *Proc Natl Acad Sci USA.* 2001;98:5572–5577.

34. Timmers, AM, Zhang H, Squitier A, et al. Subretinal injections in rodent eyes: effects on electrophysiology and histology of rat retina. *Mol Vis.* 2000;7:131–137.

35. Faktorovich EG, Steinberg RH, Yasumura D, et al. Photoreceptor degeneration in inherited dystrophy delayed by the basic fibroblast growth factor. *Nature.* 1990;347:83–86.

36. Birikh KR, Heaton PA, Eckstein F. The structure, function and application of the hammerhead ribozyme [review] *Eur J Biochem.* 1997;245:1–16.

37. Chartrand P, Leclerc F, Cedergren R. Relating conformation, $Mg2+$ binding, and functional group modification in the hammerhead ribozyme. *RNA.* 1997;3:692–696.

38. Heidenreich O, Kang SH, Brown DA, et al. Ribozyme-mediated RNA degradation in nuclei suspension. *Nucleic Acids Res.* 1995;23:2223–2228.

39. McLaughlin ME, Sandberg MA, Berson EL, Dryja TP. Recessive mutations in the gene encoding the beta-subunit of rod phosphodiesterase in patients with retinitis pigmentosa. *Nat Genet.* 1993;4:130–134.

40. Clarke G, Collins RA, Leavitt BR, et al. A one-hit model of cell death in inherited neuronal degenerations. *Nature.* 2000;406:195–199.

41. Acland GM, Aguirre GD, Ray J, et al. Gene therapy restores vision in a canine model of childhood blindness. *Nat Genet.* 2001;28:92–95.

42. Weber M, Rabinowitz J, Provost N, et al. Recombinant adeno-associated virus serotype 4 mediates unique and exclusive long-term transduction of retinal pigmented epithelium in rat, dog, and nonhuman primate after subretinal delivery, *Mol Ther.* 2003;7:774–781.

43. Surace EM, Auricchio A, Reich SJ, et al. Delivery of adeno-associated virus vectors to the fetal retina: impact of viral capsid proteins on retinal neuronal progenitor transduction. *J Virol.* 2003;77:7957–7963.

44. Lewin AS, Hauswirth WW. Ribozyme gene therapy: applications for molecular medicine [review]. *Trends Mol Med.* 2001;7:221–228.

45. Millington-Ward S, O'Neill B, Tuohy G, et al. Strategems in vitro for gene therapies directed to dominant mutations. *Hum Mol Genet.* 1997;6:1415–1426.